

*Mike Cox<sup>1)</sup>*

*1) School of Psychology,  
Newcastle University,  
Newcastle upon Tyne,  
NE1 7RU,  
England.  
Mike.cox@ncl.ac.uk*

## **A Numerical Method For Modelling The Parameters $\lambda$ and $\Delta$ Of An EWMA Chart**

**Abstract:** *The exponentially weighted moving average chart (EWMA) is widely employed in quality control to monitor a process or to evaluate historic data. EWMA charts are designed to exhibit acceptable average run lengths both when the process is in and out of control. This paper introduces a functional technique for generating the parameters  $\lambda$  and  $\Delta$  for such a chart that will have specified average run lengths. The parameters are estimated using regression plus an artificial neural network.*

**Keywords:** *ARL, average run length, EWMA chart, Exponentially Weighted Moving Average chart, neural network, parameter estimation, SPC, statistical process control*

### **1. INTRODUCTION**

Control charts are often employed to detect changes in a process mean over time. In the traditional approach, a sample is drawn and the sample mean ( $\bar{x}$ ) is calculated and plotted on a Shewhart  $\bar{X}$ -chart having control limits that depict the extremes of pure chance fluctuations. A point inside the limits suggests that the process is on target. While a Shewhart  $\bar{X}$ -chart is relatively easy to use and interpret, a cumulative sum (CUSUM) chart (Woodall, 1986) is more capable of detecting small changes in the process mean, as well as indicating the time when the production line goes “out of control”. Faster detection of significant changes means tighter control if corrective action is to be taken promptly.

Like Shewhart  $\bar{X}$  and CUSUM control schemes, an exponentially weighted moving average (EWMA) control scheme is easy to implement and interpret. The ability of the EWMA chart to detect small shifts in the process mean is

on a par with the CUSUM chart and superior to the Shewhart  $\bar{X}$ -chart. It has been argued (Lucas and Saccucci, 1990) that the EWMA chart is simpler to explain to the lay user than the CUSUM chart, by noting its similarity to the classical Shewhart  $\bar{X}$ -chart. Both the CUSUM and EWMA charts are more suitable for single sampling schemes.

A control chart procedure has been proposed for which the Shewhart  $\bar{X}$ -chart, the cumulative sum chart and the exponentially weighted moving average chart are special cases. The procedures for constructing these charts have been described by Champ et al. (1991).

Interest in the EWMA chart is reflected in the numerous papers employing the technique. The construction and performance of these charts has been discussed (Chan and Zhang, 2000 and Jones et al., 2001). Jensen et al. (2006) wrote a recent review of the area, including EWMA charts, which should probably be read in conjunction with Woodall (2000) who examined a number

of active questions on this topic. For those interested in applications, particularly within the health care industry see Woodall (2006). What was omitted from these works was a method, beyond the traditional nomogram (a graphical technique) for estimating the charts parameters. It is this problem that is addressed here. A spreadsheet is introduced as an aid to rapid calculation of the desired parameters.

The first section introduces the key notation, which is used to introduce the generalised control chart. Interest then centres on the Exponentially Weighted Moving Average chart that is central to this work and is defined employing two parameters  $\lambda$  and  $\Delta$ . The traditional approach to estimate these parameters, via a nomogram is discussed; it is argued that this method is inaccurate and out dated. A novel approach is adopted using a polynomial to estimate the first parameter ( $\lambda$ ) and a neural network to estimate the second ( $\Delta$ ). Finally a simple spreadsheet is developed to evaluate both parameters in the hope that this simple realisation will assist in the more ready adoption of this line of attack.

The formal background to the problem is now introduced.

## 2. BACKGROUND TO THE PROBLEM

Assume a sampled batch has a true mean  $\mu$ . Let  $\tau$  be an acceptable target value for  $\mu$ ; therefore a batch is acceptable if  $\mu = \tau$ . If a sample is rejected when, in fact, the mean is  $\mu = \tau$ , this is unfair to the producer. This producers risk is also referred to as a Type I error or simply denoted by a probability  $\alpha$ . Conversely, if a sample is accepted when, in fact, the mean is  $\mu \neq \tau$  this is unfair to the consumer. This consumer's risk is also referred to as a Type II error or simply denoted by a probability  $\beta$ . The difference

between  $\mu$  and  $\tau$  is the drift  $\Delta$  ( $\Delta = \tau - \mu$ ). The sample size and control limits may be selected to obtain an in control average run length for a specified  $\Delta$ .

The average run length (ARL) for a given  $\Delta$  gives the average number of batches sampled until one is rejected. The ARL is dependent on the selected parameters and is an important factor in selecting a control chart. The plan (the sample size and control limits) is usually chosen so that the ARL is large when the process is in control (acceptable ARL denoted by  $L_a$ ), and small when the process changes by  $\Delta$  (out of control or rejected ARL denoted by  $L_r$ ). The criteria are acceptable risks of incorrect actions ( $\alpha$  and  $\beta$ ), expected average quality levels (percent nonconforming) reaching the customer and expected average inspection loads (designed to detect nonconforming items).

The charts considered in this paper examine the sample mean. In a process the mean might appear acceptable, but there could be a change in the inherent process variation. To monitor this variability a Shewhart range chart should also be utilised (Cox, 1989).

The notation associated with a generalised chart is now developed.

## 3. THE GENERALISED CONTROL CHART

Assume that the individual random variables are normally distributed with mean  $\mu$  and variance  $\sigma^2$ , that is  $x \sim \phi(\mu, \sigma^2)$ . Let  $\bar{x}_t$  be the mean of a random sample of  $n$  observations during the time interval,  $t$ . Then  $\bar{x}_t$  is normally

distributed:  $\bar{x}_t \sim \phi\left(\mu, \frac{\sigma^2}{n}\right)$ . For

simplicity, all charts will be constructed

for a standard normal variable  $z_t = \frac{\bar{x}_t - \mu}{\sigma/\sqrt{n}}$

therefore  $z_t \sim \phi(0,1)$ .

The generalised procedure (Champ et al., 1991) is based on the cumulative values,

$$U_t = \max\{-a_0, a_1 U_{t-1} + a_2 z_t - a_3\},$$

$$U_0 = a_4$$

$$L_t = \min\{b_0, b_1 L_{t-1} + b_2 z_t + b_3\},$$

$$L_0 = -b_4$$

where the values of the parameters are chosen to be non-negative ( $a_2$  and  $b_2$  must be positive).

For the upper chart the key parameters are  $(a_0, a_1, a_2, a_3)$ , for the traditional Shewhart chart these are  $(0, 0, 1, 0)$ , for the CUSUM  $(0, 1, 1, k)$  and for the EWMA  $(0, 1 - \lambda, \lambda, 0)$ , adopting the usual notation, for further details see Cox (1999).

The two-sided generalised control chart gives an out of control signal as soon as either  $U_t \geq a_5$  or  $L_t \leq -b_5$ . For companion Shewhart  $\bar{X}$ -charts, additional limiting values  $a_6$  and  $b_6$  are used to indicate whenever either  $z_t \geq a_6$  or  $z_t \leq -b_6$ . These 14 parameters provide charts with a great flexibility for detecting changes in  $\mu$ . The parameters are chosen to provide signals for a shift of a given magnitude in  $\mu$  with desired ARLs.

The parameters  $a_4$  and  $b_4$  provide a head start feature, designed to detect initial out of control conditions more rapidly, negated by setting  $a_4 = b_4 = 0$ . The head start, or fast initial response, enhances the performance of the control chart. Initially, and after an out of control signal, the cumulative values are initialised at  $a_4$  and  $-b_4$ . If the process is in control, the head start parameters have little effect; however, for an out of control process, faster indication is given with a non-zero head start. Typically,  $0 \leq a_4 \leq a_5$  and  $a_4$  is often

placed at  $\frac{1}{2} a_5$  (similarly for  $b_4$ ). One-sided charts can be produced by setting  $a_5 = a_6 = \infty$ , or  $b_5 = b_6 = \infty$ .

The parameters that produce the traditional EWMA charts from the general scheme are now presented.

#### 4. EXPONENTIALLY WEIGHTED MOVING AVERAGE CHART

Following Lucas and Saccucci (1990), the variables for an EWMA chart are

$$U_t = \max\{0, (1 - \lambda)U_{t-1} + \lambda z_t\}, U_0 = 0$$

$$L_t = \min\{0, (1 - \lambda)L_{t-1} + \lambda z_t\}, L_0 = 0$$

with  $0 < \lambda \leq 1$ . The weighting parameter,  $\lambda$ , is chosen to give an appropriate average run length and is discussed further below. In this case

$$a_5 = b_5 = \Phi^{-1}(0.999) \frac{\sigma}{\sqrt{n}} \sqrt{\frac{\lambda}{2 - \lambda}}$$

Usually  $\lambda$  is chosen in the interval  $[0.05, 0.25]$  with central values being more usual. Smaller values of  $\lambda$  are employed to detect smaller shifts. For  $\lambda > 0.1$  the EWMA chart is often superior to the CUSUM chart in detecting large shifts (Montgomery, 2005).

Some aids to parameter estimation for an EWMA chart have been published (Roberts, 1959). A nomogram is a graph with several scales designed so that placing a ruler on the plot cuts the scales at related values of the variables. It is very much a graphical method with all its inherent inaccuracies further jeopardised by employing a straight edge to indicate the desired values. Roberts (1959) employed simulation techniques while Crowder (1989) numerically evaluated the integral equation to derive the nomograms

required. Since the nomogram approach cannot be readily automated it is not studied in great depth here.

A partial solution of the problem addressed here was presented by Lucas and Saccucci (1990) (see their Table 3) who adopted a Markov chain approach, following Brook and Evans (1972). Their scheme is relatively complex and involves reference to additional tables (Lucas and Saccucci, 1987). Unfortunately the method is restricted to the parameters and ARL values summarised in the table they present. The approach adopted here is far more flexible.

To illustrate the shortcomings of the traditional nomogram, the estimates required to produce the figure are calculated and the plot presented.

## 5. NOMOGRAM

In an early paper describing these charts (Roberts, 1959) produced a nomogram for the dimensionless case

$$a_5 = b_5 = 3\sqrt{\frac{\lambda}{2-\lambda}} \text{ with } n = \sigma = 1; \text{ this is}$$

re-evaluated and presented in Figure 1. As in the original work, for clarity, a logarithmic scale is adopted for the ordinate. The evaluation of the ARL values needed to produce this plot has been described elsewhere ((Cox, 1999) enhanced with Gaussian knot points for the numerical integration). So given  $\lambda$  and  $\Delta$ ,  $L_r$  may be evaluated in this case. The range selected for  $\lambda$  and  $\Delta$  were chosen to match those of Roberts (1959). A great deal of uncertainty is associated with estimating  $\Delta$  from this figure due to the proximity of the curves for  $\lambda$ .

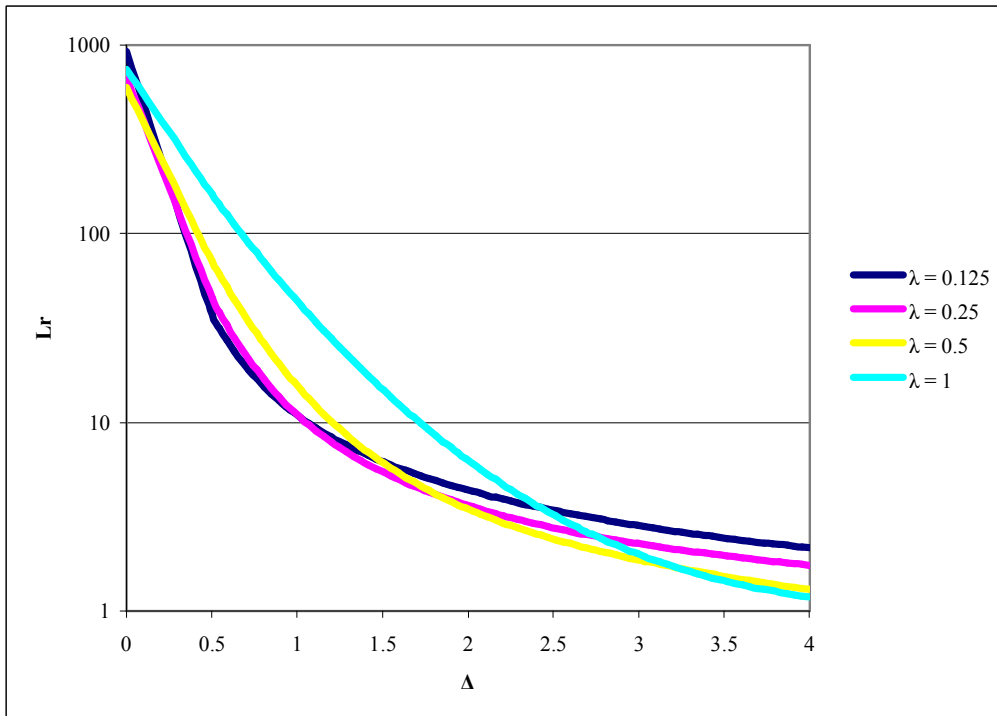


Figure 1  $L_r(\Delta)$  For Given  $\lambda$

These nomograms have not been as readily adopted as those for the CUSUM chart (Kemp, 1962). The reason is clear from the figure. The curves are so close that parameter selection for the desired  $L_r$  is impractical. If  $\Delta$  is identified from the figure, the result is seen to be effectively independent of  $\lambda$ . Recall that small values are desirable  $0.05 \leq \lambda \leq 0.25$ .

A superior method is now introduced, a polynomial approach is used to estimate  $\lambda$  and a neural network to estimate  $\Delta$ .

### 6. A POLYNOMIAL TO ESTIMATE $\Delta$

In the following calculations, for each value of  $a_5$  investigated 6,561 examples are examined with  $0.01 \leq \lambda \leq 1$  and  $0.5 \leq \Delta \leq 4$ . In each case 30 Gaussian knot points were employed in the numerical

integration to provide the estimates (Cox, 1999). Defining  $a_5 = c_5 \sqrt{\frac{\lambda}{2-\lambda}}$ , setting  $c_5 = 3$  results in the case presented in Figure 1. The dimensionless case is retained by selecting  $n = \sigma = 1$ . To assist in parameter selection for various values of  $c_5$ , limits (Table 1) on  $L_a$ , corresponding to  $\Delta = 0$ , are employed.

**Table 1 Acceptable Ranges For  $L_a$**

Given $c_5$		1	1.5	2	2.5	3
$L_a$		[6.3, 83]	[15, 221]	[44, 572]	[161, 1,632]	[741, 5,647]

Since  $L_a$  is independent of  $\Delta$  (it corresponds to  $\Delta = 0$ ) it provides an estimate of  $\lambda$ . The corresponding curves are presented in Figure 2.

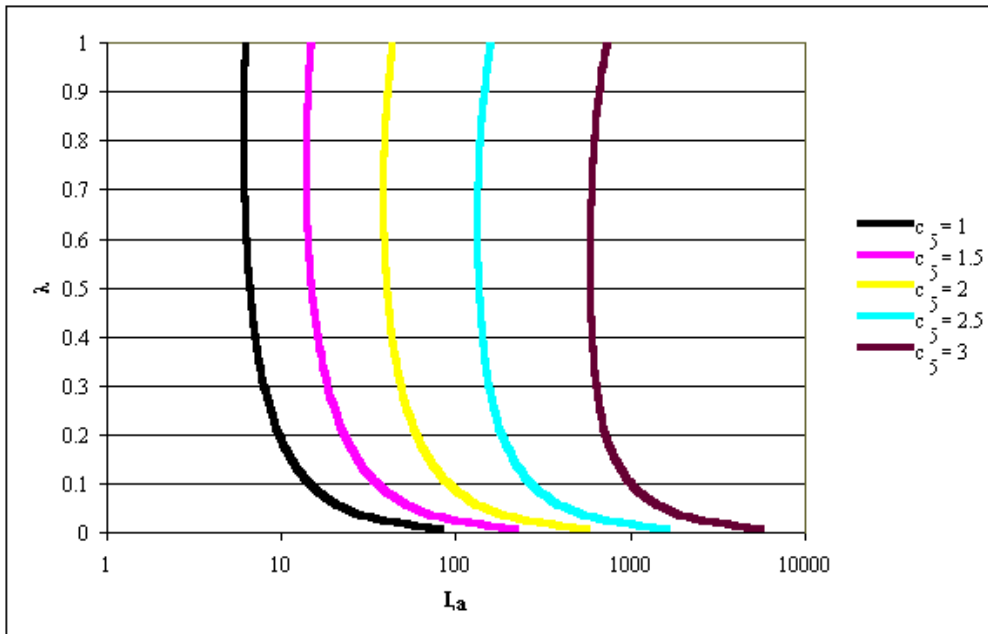


**Figure 2 -  $L_a(\lambda)$  For Given  $c_5$**

To move away from the graphical approach it is necessary to replace each of these curves with a function. In view of

their smooth profile a simple polynomial is employed.

In each case the plots exhibit a long tail with a slight increase in  $L_a$  as  $\lambda$  approaches 1. In view of this the extreme estimate of  $L_a$ , corresponding to  $\lambda = 1$ , is adopted as the minimum acceptable value. The first estimate of  $\lambda$  that corresponds to this estimate is denoted  $\lambda_{\max}$  in Table 2 and provides a limit on the applicability of the fitting polynomial, which is adequate for all the cases considered here.

On logarithmic axis the curves are relatively easy to fit. The logarithmic transform is also adopted to provide consistency with the fits developed below. In an attempt to clarify the situation, the

coefficients that estimate  $\ln(\lambda)$  given  $\ln(L_a)$  are defined in the following polynomial

$$\ln(\lambda) = b_0 + b_1 \ln(L_a) + b_2 \ln(L_a)^2.$$

For given  $c_5$  these, and their range of applicability  $(0, \lambda_{\max})$ , and the corresponding  $R^2$  value for the 60 points employed in the fit are presented in Table 2. As an aid to interpreting the accuracy of any estimates made some descriptive statistics have also been included.

**Table 2 Fitting Coefficients For  $\lambda$  Given  $L_a$**

$c_5$	1	1.5	2	2.5	3	Maximum
$\lambda_{\max}$	0.64	0.51	0.38	0.27	0.18	
$b_0$	4.7807	6.0438	9.0176	13.6997	20.5488	
$b_1$	-3.4949	-3.0681	-3.4036	-4.0329	-4.8528	
$b_2$	0.3171	0.2055	0.1995	0.2114	0.225	
$R^2$	99.50%	99.80%	99.90%	99.90%	99.90%	
Minimum	-0.1337	-0.0732	-0.0548	-0.0371	-0.0249	-0.0249
Lower Quartile	-0.0605	-0.0325	-0.0295	-0.0273	-0.0206	-0.0206
Median	-0.0142	-0.0106	-0.0088	-0.0071	-0.0089	-0.0071
Upper Quartile	0.0583	0.0314	0.0275	0.0268	0.0248	0.0583
Maximum	0.1366	0.0769	0.0593	0.0532	0.0394	0.1366
Inter Quartile Range	0.1188	0.0639	0.057	0.0541	0.0453	0.1188
Standard Deviation	0.067	0.0376	0.0328	0.0296	0.023	0.067

The  $R^2$  values support the reliability of the fit and hence, for selected  $c_5$  and desired  $L_a$ ,  $\lambda$  may be reliably estimated. Further support, during the analysis stage, was given by the proximity of the confidence limits to the fitted line.

Estimation of the remaining parameter,  $\Delta$ , will now be addressed via a neural network.

## 7. A NEURAL NETWORK TO ESTIMATE $\Delta$

The remaining problem is to employ the desired values of  $L_a$  and  $L_r$  to estimate  $\Delta$ . In this case  $L_a$  acts as a proxy for  $\lambda$ . It was hoped to again employ a polynomial approximation, however the complexity of this problem is illustrated by Figures 3, 4, 5 and 6, which preclude this. These figures

present contour plots, with  $\Delta$  as the altitude. A polynomial fit would suffice if, for example, the map exhibited a simple hill or valley, but unfortunately this is

clearly not the case. For example with  $c_5 = 1$ , contours of  $\Delta$  against axis of  $L_a$  and  $L_r$  are presented.

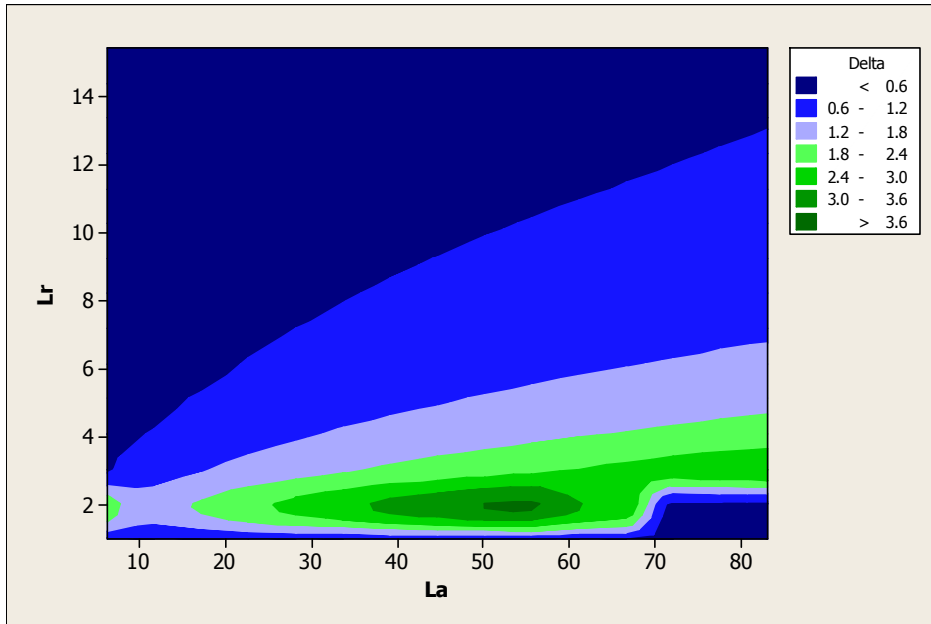


Figure 3 Contours For  $\Delta$  Given  $L_a$  and  $L_r$  For  $c_5 = 1$

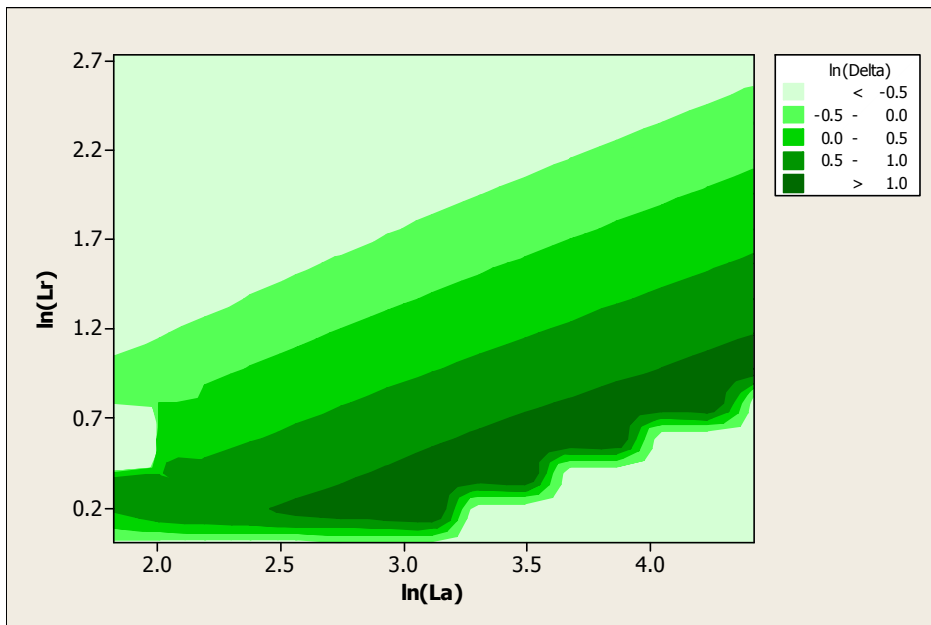


Figure 4 Contours For  $\Delta$  Given  $\ln(L_a)$  and  $\ln(L_r)$  For  $c_5 = 1$

As with the estimation of  $\lambda$  logarithmic variables are adopted in an attempt to clarify the situation.

Unfortunately the landscape while exhibiting some linear features has a scalloped edge on the south face of the

peak ( $\ln(\Delta) > 1$ ).

It may be that the case considered ( $c_5 = 1$ ) was unusual, however similar complexity is exhibited for the extreme value of  $c_5 = 3$ .

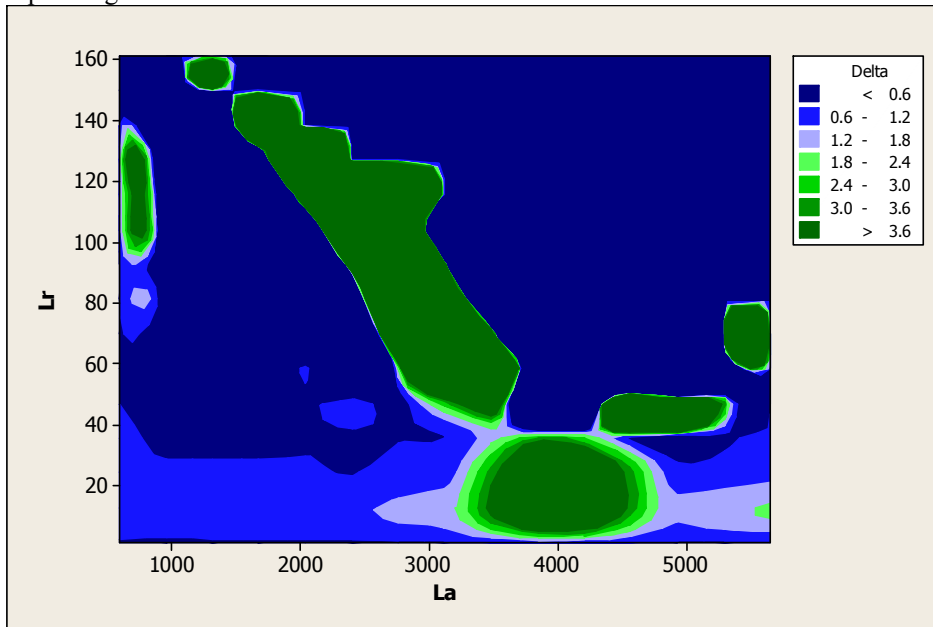


Figure 5 Contours For  $\Delta$  Given  $L_a$  and  $L_r$  For  $c_5 = 3$

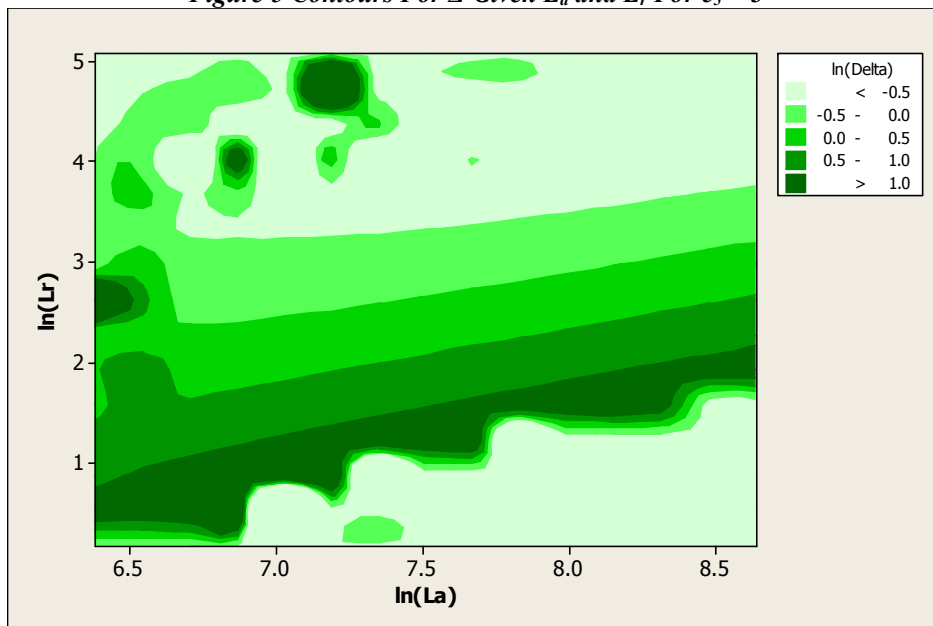


Figure 6 Contours For  $\Delta$  Given  $\ln(L_a)$  and  $\ln(L_r)$  For  $c_5 = 3$

For completeness, logarithmic transformations are again employed; hoping that some clear structure might be exhibited.

It is tempting to assume that the irregular surfaces depicted are a result of numerical imprecision. As a check the number of knot points for the numerical integration was doubled, this produced no discernable difference.

In view of this complex behaviour neural networks are employed which are ideal for modelling in situations like this. A simple neural network ((Cox, 2001) and references therein) with 2 inputs ( $x_1$  and  $x_2$ ), a single hidden layer ( $x_3$ ,  $x_4$  and  $x_5$ ) used to predict a single output ( $x_6$ ) may be constructed. The functions and variables employed are displayed in Table 3.

**Table 3 Functions Employed In The Neural Network**

Input for $x_1$	$x_1 = \ln(L_r)$
Input for $x_2$	$x_2 = \ln(L_a)$
Sigmoid transfer function	$\phi_1(x) = \frac{1 - e^{-x}}{2(1 + e^{-x})}$
Linear transfer function	$\phi_0(x) = x$
Transfer function for $x_3$	$x_3 = \phi_1(x_1 a_{1,3} + x_2 a_{2,3} + u_3)$
Transfer function for $x_4$	$x_4 = \phi_1(x_1 a_{1,4} + x_2 a_{2,4} + u_4)$
Transfer function for $x_5$	$x_5 = \phi_1(x_1 a_{1,5} + x_2 a_{2,5} + u_5)$
Transfer function for $x_6$	$x_6 = \phi_0(x_3 a_{3,6} + x_4 a_{4,6} + x_5 a_{5,6} + u_6) = \ln(\Delta)$

**Table 4 Fitted Coefficients For The Neural Network**

$c_s$	1	1.5	2	2.5	3
$u_3$	0.2074	2.6386	1.4323	-2.0037	-11.5348
$a_{1,3}$	-10.6578	-1.3392	1.0377	2.5924	1.4428
$a_{2,3}$	-0.7335	-0.1137	-0.9012	-0.2697	1.1120
$u_4$	1.9953	0.5096	8.7847	6.4794	15.5815
$a_{1,4}$	0.3024	5.5010	2.6155	-1.1498	2.8244
$a_{2,4}$	-0.9767	0.2699	-2.3520	-0.7061	-2.8026
$u_5$	-0.7748	-3.0540	4.6535	-8.3862	15.7251
$a_{1,5}$	1.9116	-0.6320	-0.9311	-1.4227	1.1294
$a_{2,5}$	-0.4816	1.0026	-0.6254	1.6960	-2.1119
$u_6$	1.0920	1.1709	0.2200	0.7376	0.9502
$a_{3,6}$	2.2746	2.2561	-1.6853	0.0623	-1.2149
$a_{4,6}$	-1.7222	-1.9634	-1.1741	1.6097	-0.8425
$a_{5,6}$	-2.5229	2.6065	1.2613	2.0580	-1.1682

The software utilised to calculate the weights and thresholds is freely available in the public domain (Goodman, 2001) (A downloadable zip file contains executable, source code, a manual and an example. The programme will run under the Windows operating system, but does not

possess any of the systems flexibility in file handling and parameter input.). The resulting coefficients are displayed in Table 4.

As an indication of the value of the proposed model, a general second order polynomial was also fitted to the data.

Although the fits resulted in excellent R<sup>2</sup> values, in all cases the fit was inferior to that obtained from the neural network. For the case c<sub>5</sub> = 1 using the 6,561 points,

relevant descriptive statistics for the fitting errors in the two cases are displayed in Table 5.

**Table 5 Errors For The Neural And Polynomial Approximations For c<sub>5</sub> = 1**

	Error in Δ		Percentage Error in Δ	
	Neural	Polynomial	Neural	Polynomial
<b>Minimum</b>	-0.46	-0.81	-11	-37
<b>Lower Quartile</b>	-0.03	-0.07	-2	-5
<b>Median</b>	0.00	0.01	0	1
<b>Upper Quartile</b>	0.05	0.15	2	7
<b>Maximum</b>	0.22	0.30	17	21
<b>Inter Quartile Range</b>	0.08	0.23	4	12
<b>Standard Deviation</b>	0.1033	0.2225		

Thus for virtually every measure evaluated the neural network is superior. The sole disadvantage of the neural network approach is that it does not provide any indication of expected errors that might be associated with a parameter estimate. However some indication may be obtained from the descriptive statistics included in Table 5.

In general the estimates of λ are fairly accurate, those of Δ slightly less so, as revealed by a direct solution of the numerical problem. The approximate values from the polynomial (Table 2) and the neural network (Table 4) provide starting values for the simplex procedure (Nelder and Mead, 1965) to directly solve the numerical problem of estimating λ and Δ for given L<sub>a</sub>, L<sub>r</sub> and c<sub>5</sub> (note that a<sub>1</sub>, a<sub>2</sub>, a<sub>5</sub> all depend on λ).

The estimated acceptable average run length is ARL(a<sub>0</sub>,a<sub>1</sub>,a<sub>2</sub>,a<sub>3</sub>,a<sub>4</sub>,a<sub>5</sub>) with density function φ(z) and is denoted by ARL<sub>a</sub>. While the rejection value corresponds to ARL(a<sub>0</sub>,a<sub>1</sub>,a<sub>2</sub>,a<sub>3</sub>,a<sub>4</sub>,a<sub>5</sub>) with a shift in the density function φ(z - Δ) and is denoted by ARL<sub>r</sub>. The relevant equations to derive the ARL are presented in the appendix of Cox (1999). Here the

procedure is enhanced with Gaussian quadrature for the numerical integration, employing 30 knot points. Algorithm's to calculate the Gauss-Legendre weights and abscissa are readily available (Press et al., 1992). The estimates (λ, Δ) are obtained by minimising the function

$$\frac{(L_a - ARL_a)^2}{L_a} + \frac{(L_r - ARL_r)^2}{L_r}$$

that was

designed to resemble a χ<sup>2</sup> statistic and take into account the possible difference in magnitude between L<sub>a</sub> and L<sub>r</sub>.

The difficulty in evaluating a precise value of Δ is unsurprising given the proximity of the curves in Figure 1. For instance, in the case c<sub>5</sub> = 3, L<sub>r</sub> = 3 and L<sub>a</sub> = 1000, the approximate values employing the equations developed here are λ = 0.11 and Δ = 2.99 (see Table 6 below). While the exact calculation gives λ = 0.10 and Δ = 3.00, not a major discrepancy.

Since some of the equations are a little complex, a spreadsheet aid to the calculation of λ and Δ is now presented.

### 8. A SPREADSHEET TO EVALUATE $\lambda$ AND $\Delta$

A spreadsheet was constructed to perform the basic evaluations; the foreground is displayed in Table 6.

It is a simple matter to enter coefficients for other values of  $c_5$ . It evaluates the previously considered case ( $c_5 = 3$ ,  $L_r = 3$  and  $L_a = 1000$ ).

### 9. CONCLUSIONS

EWMA charts are widely used in quality control, both in the traditional industrial sector and within areas such as health care (Woodall, 2006). They are particularly efficient in detecting small shifts in the process mean. Control charts being a graphical method mean that a process shift of the plotted points is readily observed.

**Table 6 Spreadsheet Values For  $c_5 = 3$**

	A	B	C	D	E	F	G	H
1	<b>A Neural Net Modelling The Parameters Of An EWMA Chart</b>							
2	File	EWMA_Neural.xls						
3								
4	<b>Input ARL's</b>				<b>EWMA Parameters</b>			
5	$L_r$	3	$L_a$	1000	$\lambda$	0.11	$\Delta$	2.99
6								
7	<b>Constants and Outputs</b>							
8	$x_1$	1.10	$x_2$	6.91				
9								
10	$a_{1,3}$	1.44	$a_{2,3}$	1.11	$u_3$	-11.53		
11	$x_3$	-0.41						
12								
13	$a_{1,4}$	2.82	$a_{2,4}$	-2.80	$u_4$	15.58		
14	$x_4$	-0.16						
15								
16	$a_{1,5}$	1.13	$a_{2,5}$	-2.11	$u_5$	15.73		
17	$x_5$	0.42						
18								
19	$a_{3,6}$	-1.21	$a_{4,6}$	-0.84	$a_{5,6}$	-1.17	$u_6$	0.95
20	$x_6$	1.10						
21								
22	$b_0$	20.55	$b_1$	-4.85	$b_2$	0.22		

A simple polynomial plus a neural network adopted here yields a series of equations, which can be evaluated to quickly provide estimates of the parameters  $\lambda$  and  $\Delta$  for an EWMA chart with desired average run lengths. The approach is reasonably accurate and more immediate than the alternate method employing nomograms. If greater precision is desired, then a larger structure for the neural network could be employed, or a direct numerical approach (as described above) adopted using the

polynomial and neural network estimates as starting points. However since the control charts are only based on estimated values (underlying population mean and standard deviation (Jensen et al., 2006)) then excessive accuracy need not be demanded of the chart parameters.

**REFERENCES:**

- [1] Brook D. and Evans D.A., (1972) An Approach To The Probability Distribution Of CUSUM Run Length, *Biometrika*, 59, pp. 539-549.
- [2] Champ C.W., Woodall, W.H. and Mohsen, H.A., (1991) A Generalised Quality Control Procedure, *Statistics and Probability Letters*, 11, pp. 211-218.
- [3] Chan L.K. and Zhang, J., (2000) Some Issues In The Design Of EWMA Charts, *Communications in Statistics – Simulation and Computation*, 29, pp. 207-217.
- [4] Cox M.A.A. (1989) Control Charts On Spreadsheets; A Tutorial Guide Or A Poor Mans Persuader, *Quality Engineering*, 1, pp. 19-39.
- [5] Cox M.A.A. (1999) Towards The Implementation Of A Universal Control Chart And Estimation Of Its Average Run Length Using A Spreadsheet, *Quality Engineering*, 11, pp. 511-536.
- [6] Cox M.A.A. (2001) Towards The Implementation Of A Universal Control Chart And Estimation Of Its Average Run Length Using A Spreadsheet: An Artificial Neural Network Is Used To Model The Parameters In A Special Case, *Journal of Applied Statistics*, 28(3), pp. 353-364.
- [7] Crowder S.V. (1989) Design of Exponentially Weighted Moving Average Schemes, *Journal of Quality Technology*, 21(3), pp. 155-162.
- [8] Goodman P.H. (2001) NevProp Software, Version 4, University of Nevada: Reno, NV, URL: <http://brain.cs.unr.edu/publications/NevProp.zip> (accessed July 2010).
- [9] Jensen W.A., Jones-Farmer, L.A., Champ, C.W. and Woodall, W.H. (2006) Effects Of Parameter Estimation On Control Chart Properties: A Literature Review, *Journal of Quality Technology*, 38, pp. 349-364.
- [10] Jones L.A., Champ, C.W. and Rigdon, S.E. (2001) The Performance Of Exponentially Weighted Moving Average Charts With Estimated Parameters, *Technometrics*, 43, pp. 156-167.
- [11] Kemp K.W. (1962) The Use Of Cumulative Sums For Sampling Inspection Schemes, *Applied Statistics*, 11, pp. 16-31.
- [12] Lucas J.M. and Saccucci M.S. (1987) Exponentially Weighted Moving Average Control Schemes, Properties and Enhancements, Faculty Working Series Papers 87-5, Drexel University, Dept. of Quantitative Methods.
- [13] Lucas J.M. and Saccucci M.S. (1990) Exponentially Weighted Moving Average Control Schemes, Properties and Enhancements, *Technometrics*, 32, pp. 1-29.
- [14] Montgomery D.C. (2005) Introduction to Statistical Quality Control, 5<sup>th</sup> Ed., John Wiley: Hoboken, N.J.
- [15] Nelder J.A. and Mead R. (1965) A Simplex Method For Function Minimisation, *Computer Journal*, 7, pp. 308-313.
- [16] Press, W.H., Flannery, B.P., Teukolsky, S.A. and Vetterling, W.T., ‘Numerical recipes in Fortran: the art of scientific computing’, Second Edition, Cambridge University Press, Cambridge, England (1992). Also see <http://www.nrbook.com/nr3/> (accessed July 2010).
- [17] Roberts S.W. (1959) Control Chart Tests Based On Geometric Moving Averages, *Technometrics*, 1, pp. 239-250.
- [18] Woodall W.H. (1986) The Design Of CUSUM Quality Control Charts, *Journal of Quality Technology*, 18, pp. 99-102.
- [19] Woodall W.H., (2000) Controversies And Contradictions In Statistical Process Control, *Journal of Quality Technology*, 32, pp. 341-350.
- [20] Woodall W.H., (2006) The Use Of Control Charts In Health-Care And Public-Health Surveillance, *Journal of Quality Technology*, 38, pp. 89-104.